Characterization of fluorescence lifetime of organic fluorophores for molecular imaging in the shortwave infrared window

Luis Chavez,[*,†] **Shan Gao**,[†] **and Xavier Intes**
Rensselaer Polytechnic Institute, Center for Modeling, Simulation and Imaging in Medicine, Troy, New York, United States

Abstract

Significance: Fluorescence lifetime imaging in the shortwave infrared (SWIR) is expected to enable high-resolution multiplexed molecular imaging in highly scattering tissue.

Aim: To characterize the brightness and fluorescence lifetime of commercially available organic SWIR fluorophores and benchmark them against the tail emission of conventional NIR-excited probes.

Approach: Characterization was performed through our established time-domain mesoscopic fluorescence molecular tomography system integrated around a time-correlated single-photon counting-single-photon avalanche diode array. Brightness and fluorescence lifetime were measured for NIR and SWIR probes >1000 nm. Simultaneous probe imaging was then performed to assess their potential for multiplexed studies.

Results: The NIR probes outperformed SWIR probes in brightness while the mean fluorescence lifetimes of the SWIR probes were extremely short. The phantom study demonstrated the feasibility of lifetime multiplexing in the SWIR window with both NIR and SWIR probes.

Conclusions: Long-tail emission of NIR probes outperformed the SWIR probes in brightness >1000 nm. Fluorescence lifetime was readily detectable in the SWIR window, where the SWIR probes showed shorter lifetimes compared to the NIR probes. We demonstrate the feasibility of lifetime multiplexing in the SWIR window, which paves the way for *in vivo* multiplexed studies of intact tissues at improved resolution.

 [DOI: 10.1117/1.JBO.28.9.094806]

Keywords: shortwave infrared; fluorescence lifetime imaging; lifetime multiplexing.

Paper 220285SSR received Nov. 30, 2022; accepted for publication Mar. 24, 2023; published online Apr. 10, 2023.

1 Introduction

Fluorescence optical imaging is an invaluable research tool that allows for non-invasive monitoring of numerous biological processes in live biological systems. Thanks to its high sensitivity, continuously growing library of available probes, and ability to image multiple probes simultaneously, fluorescence optical imaging techniques in the near-infrared (NIR) spectral window (700 to 1000 nm) have found numerous preclinical and clinical applications.[1] However, the resolution of these approaches is hampered by the scattering nature of tissues. As the scattering properties of tissue follow a power law in which the wavelength is the exponent, imaging further in the red has long been expected to improve imaging resolution. Only recently, thanks to the increasing availability of indium gallium arsenide (InGaAs) sensors with extremely high quantum efficiency (>80%) in the shortwave IR (SWIR) spectral range (1000 to 2000 nm), far-red imaging *in vivo* has been demonstrated to be feasible at depths comparable to NIR methods.

*Address all correspondence to Luis Chavez, chavel2@rpi.edu
†These authors contributed equally

In conjunction with dedicated probes, SWIR imaging has been demonstrated to result in enhanced resolution,[2] especially when using nanoparticles,[3] while benefiting from lower tissue autofluorescence. However, such probes are limited to vascular imaging due to their sizes and SWIR-dedicated organic fluorophores[4] are required for enabling the vast majority of biological processes monitored by NIR probes. Alternatively, it has been proposed to acquire the long-tail spectral emission of conventional NIR-excited probes in the SWIR window.[5] Still, such approaches are limited due to the need to use long-pass filters that do not allow for spectral discrimination between molecules when multiplexed studies are involved. This drawback may be overcome using another distinctive fluorophore intrinsic property: its lifetime.

Fluorescence lifetime imaging (FLI) in the NIR window offers the ability to monitor intracellular parameters in preclinical applications,[6] including cellular metabolism[7] and pH,[8] as well as to quantify Förster resonant energy transfer for monitoring probe target engagement.[9,10] Integrating FLI into well-established intensity-based imaging systems can complement their performances; recently, our group characterized and validated scanning-based time-domain mesoscopic fluorescence molecular tomography (TD-MFMT), capable of acquiring fluorescence intensity for 3D probe reconstruction as well as resolving fluorescence lifetime information in the visible-NIR window.[11] Nevertheless, challenges in implementing FLI in SWIR arise from limitations in both SWIR-specific probes and detectors. Current studies mostly use inorganic probes that can be used for luminescence lifetime multiplexing[12] but that raise biocompatibility issues.[13] Besides, intensity in the long tail emission of NIR probes represents only a small fraction of the maximum intensity, requiring detectors with high quantum efficiency (QE) and low dark current noise for effective signal-to-noise (SNR) detection.[2] Moreover, the fluorescence lifetime of organic NIR fluorophores decreases as the wavelength approaches the SWIR window,[14] demanding systems with high temporal resolution for lifetime quantification. Furthermore, the commonly used time-resolved detectors for lifetime quantification encounter difficulties to extend their utilities in the SWIR range. Beyond the drawbacks of the mechanically fragile feature and large form factor, there are few photomultiplier tubes commercially available in the NIR, and even fewer in the SWIR.[15] Another preferred imager in the NIR—the gated CCD has its QE cutoff above 900 nm and hence hinders its implementation for longer wavelength detection. Alternatively, due to the relatively decent QE in the SWIR range and the impressive temporal resolution, silicon-based single-photon avalanche diode (SPAD) array[16] coupled with a time-correlated single-photon counting (TCSPC) module has the potential to quantify the short lifetime of the SWIR-specific fluorophores. Recently, with the development of the emerging germanium-based SPAD[17] and superconducting nanowire single-photon detector,[18] SWIR imaging applications promise to benefit from the high QE and low dark count of such detectors. Yu et al. presented a SWIR confocal FLI microscopy using a home-built superconducting single-photon nanowire (SSPD) and measured the lifetime of indocyanine green (ICG) in different biochemical buffers;[19] however, this technology is currently significantly more costly. Herein, due to the consideration of availability and cost, we report on the brightness and lifetime characteristics of ubiquitous NIR and SWIR fluorophores using the well-established silicon-based SPAD technique.

Previous research has characterized the brightness of commercially available NIR and SWIR-specific probes in the NIR-SWIR windows[2,5] and the lifetime of organic NIR fluorophores has been well documented.[13] However, there is still a lack of studies characterizing the lifetime of commercially available SWIR fluorophores. Herein, we report for the first time the lifetime characterization of SWIR-specific fluorophores IR-E1050 and IR-T1050. Additionally, we compare both brightness and lifetime of the SWIR fluorophores against the tail emission of conventional NIR fluorophores—IRDye800CW and Alexa Fluor 750—in the SWIR window by leveraging TD-MFMT system in well-plate settings. By performing phantom experiments, we demonstrate the lifetime multiplexing in the SWIR regime by distinguishing short-lifetime fluorophores and accurately quantifying the relative concentration fraction of two mixed dyes.

2 Methods and Results

To characterize the performance of NIR/SWIR fluorophores in regards to brightness and lifetime properties, we employed our established TD-MFMT system to leverage its outstanding temporal

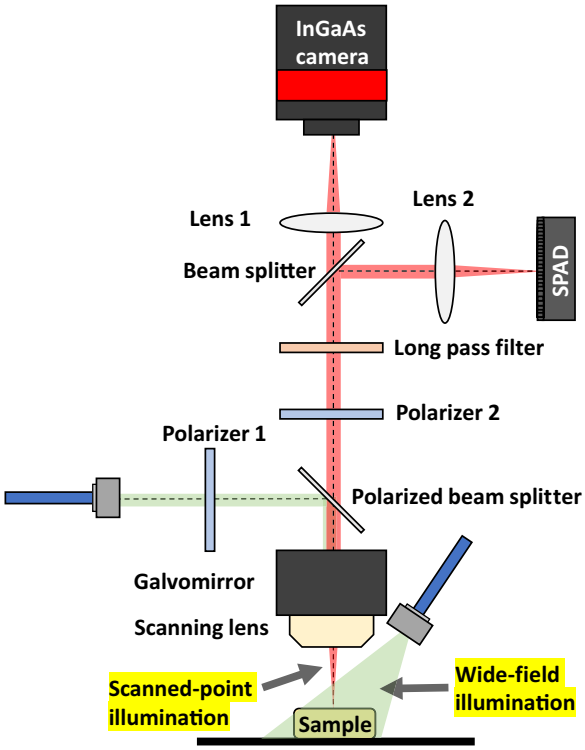

Fig. 1 Adapted TD-MFMT system schematic for SWIR lifetime characterization.[11]

resolution (up to ~90 ps of full width at half maximum of the instrument response function (IRF) and 1.6 ps time step resolution). For the NIR dyes, we selected IRDye 800CW (LI-COR Bioscience, Lincoln, Nebraska, United States) and Alexa Fluor 750 (AF750, ThermoFisher, Waltham, Massachusetts, United States) due to their ubiquitous use in the field. For the SWIR-specific fluorophores, we employed commercially available probes, IR-E1050 and IR-T1050 (Nirmidas Biotech, Mountain View, California, United States).[2] Compared to the diagram reported previously,[11] TD-MFMT system was adapted by replacing the scientific complementary metal-oxide-semiconductor (sCMOS) camera with an InGaAs camera (Owl 640 II, Raptor Photonics, United Kingdom) and switching the optics to the components with anti-reflection coatings optimized in the SWIR range (shown in Fig. 1) for optimal detection efficiency. A wide-field (WF) illumination was additionally set up for acquiring WF intensities by the InGaAs camera for brightness comparison. Sequentially, with the scanned point illumination, TD datasets were obtained by the SPAD array coupled with the TCSPC module for lifetime quantification. A tunable Ti:Sapphire pulse laser (MaiTai, Spectra-Physics, Mountain View, California, United States) is used by the WF acquisition as well as the scanning-based TD measurements producing pulses across 690 to 1040 nm.

The four fluorophores were diluted in phosphate-buffered saline solution to a concentration of 5 μM for well-plate and phantom imaging experiments. With the exception of IRDye800CW, which was excited using 775-nm wavelength, the rest of the three fluorophores were excited at 745 nm, and all four fluorophores were imaged with the same long-pass emission filter (FELH1000, Thorlabs, Newton, New Jersey, United States). The laser power was set as 6.5 and 62 mW/cm^2 for WF and TD acquisitions, respectively (well below the maximum permissible exposure instructed by the American National Standards Institute laser safety standards). Following a single shot of WF acquisition, temporal point spread functions (TPSFs) were captured at each scanning position by the SPAD and fed into a mono-exponential fitting model for the pixel-wise lifetime quantification using AlliGator (a custom software developed by X. Michalet at UCLA).[20,21] One can refer to our previous work for further details of the workflow on the TD data collection and lifetime characterization. In this work, we characterized the lifetime of AF700 accurately with nanomolar molecular concentration.[11] The WF and SPAD-based intensities measured by the InGaAs camera and the SPAD, the lifetime quantification results, as

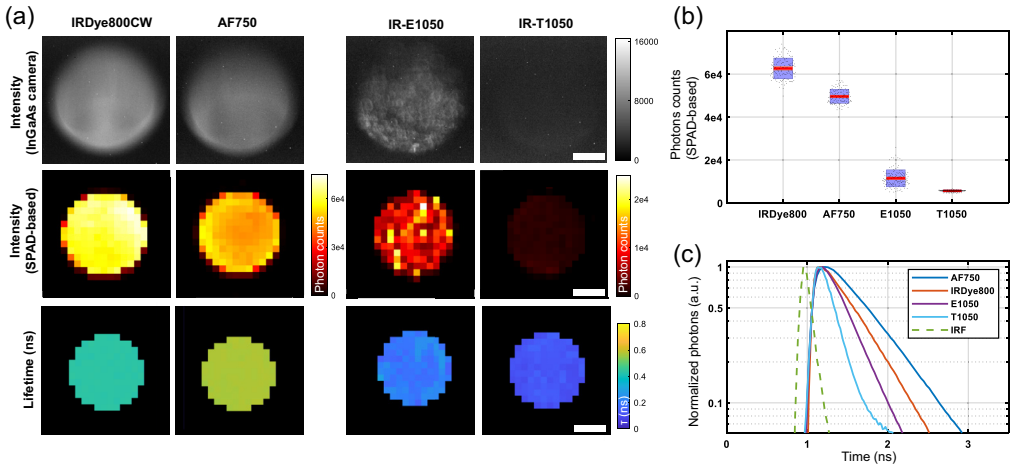

Fig. 2 Intensity comparison and lifetime quantification results with well-plate settings. (a) WF/SPAD-based intensity and lifetime maps for four fluorophores (scanning point = 20 × 20, scanning step = 250 μm, and scale bar = 1 mm). (b) Pixel-wise photon count distribution measured with SPAD in a box plot. (c) Normalized representative fluorescence decays and IRF in logarithmic scale.

well as the normalized IRF and representative decays of four fluorophores are shown in Figs. 2(a) and 2(c). Figure 2(b) illustrates the pixel-wise SPAD-based intensity distribution of the four fluorophores. Our results show that when excited at their optimal absorption wavelength, the tail emission of the NIR-excited fluorophores emitted a brighter signal compared to the SWIR fluorophores, where signal from IRDye800CW and AF750 was approximately four and three times brighter than the brightest SWIR probe, respectively. Furthermore, the characterization of the mean lifetime of the probes indicates that the SWIR probes exhibit very short lifetimes, confirming the aforementioned relationship between emission wavelength and fluorescence lifetime. The lifetime of IRDye800CW and AF750 is consistent with the results acquired in the NIR window in our former study,[21] demonstrating the system's accuracy of lifetime quantification. These findings are summarized in Table 1.

To validate the potential for multiplexed imaging using lifetime contrast while acquiring in the SWIR spectral range, a phantom was 3D printed with Rensselaer Polytechnic Institute (RPI) letter grooves [paradigm shown in Fig. 3(a)], which contains AF750, IRDye800CW, and IR-E1050 at 5 μM for letters "*R*," "*P*," and "*I*," respectively. The illumination wavelength was tuned at 750 nm for maximizing the absorption efficiency of all the fluorophores. The WF and TD datasets were captured and processed following the same imaging protocol in the well-plate experiments, though the whole sample was imaged at once using the same system settings. The results shown in Fig. 3 establish the feasibility of simultaneous detection of multiple probes in the SWIR window through multiple modalities at clinically relevant concentrations and with the same excitation setting. Intensity detection shown in Figs. 3(b) and 3(c) demonstrates that probe distribution can be readily monitored at high resolution, despite significant variations in brightness between different probes. Similarly, fluorescence lifetime quantification results shown in Fig. 3(d) illustrate the ability to quantify lifetime values accurately while using our

Table 1 Summary of fluorophore characterization (mean ± standard deviation).

Fluorophore	Brightness (10^4 photon counts)	Lifetime (ns)
IRDye800CW	6.16 ± 0.72	0.435 ± 0.004
AF750	4.88 ± 0.45	0.572 ± 0.003
IR-E1050	1.38 ± 0.39	0.206 ± 0.011
IR-T1050	0.57 ± 0.03	0.151 ± 0.007

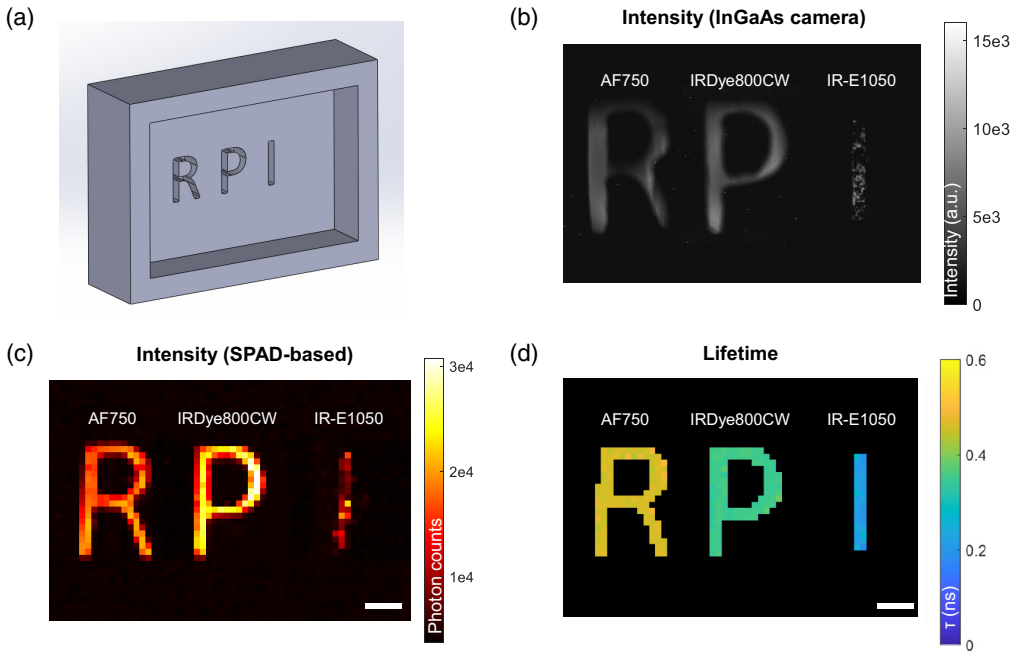

Fig. 3 Lifetime quantification by liquid phantom experiment. (a) 3D-printed RPI phantom container. (b, c) WF/SPAD-based intensity. (d) Lifetime map. (Scanning point = 40×60, scanning step = 250 μm). Scale bar = 1 mm.

SPAD-array as well as significant lifetime contrast between probes. To demonstrate the potential of using such lifetime contrast for multiplexing studies, we mixed AF750 and IR-T1050 together at different concentration ratios. 3 μM AF750 and 100 μM IR-T1050 solutions were prepared to obtain comparable intensities while using the same excitation wavelength (750-nm laser) and emission settings (long-pass filter FELH1000) aforementioned. Three wells were filled with both dyes to get a total volume of 300 μL at different volume ratios ranging from 1:1 to 3:1 (AF750: IR-T1050). TD imaging was conducted following the same protocol as previously described and the datasets were fitted using a bi-exponential decay model in AlliGator with initial lifetimes ($\tau_{AF750} = 0.57$ ns and $\tau_{T1050} = 0.15$ ns) based on the prior mono-exponential fitting results. The SPAD-based intensity maps, the amplitude fraction maps of AF750 as well as the representative TPSFs with different volume fractions are illustrated in Figs. 4(a) and 4(c). The amplitude

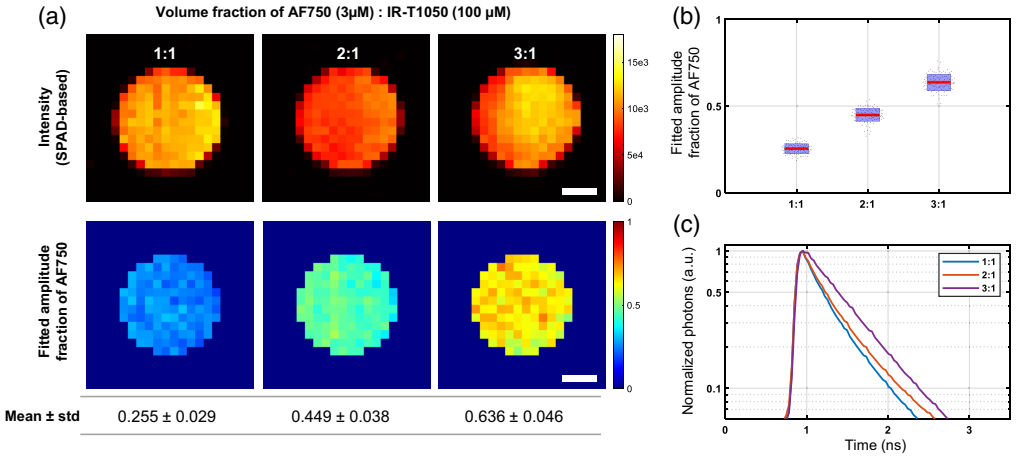

Fig. 4 Lifetime multiplexing by two fluorescence dyes. (a) SPAD-based intensity map and fitted amplitude fraction of AF750. (b) Pixel-wise distribution of fitted amplitude fraction of AF750 in a box plot. (c) Representative fitted decays. (Scanning point = 20×20, scanning step = 250 μm). Scale bar = 1 mm.

fraction was extracted from the fitting and can be correlated with the fluorophore fraction in the mixture, where the amplitude fraction of AF750 tends to increase as the volume of AF750 becomes dominant in the mixture [shown in Fig. 4(b)], thus demonstrating the potential of lifetime as a contrast mechanism to unmix fluorophores in the SWIR window while using long pass filter for optimal brightness.

3 Discussion

Concurrent monitoring of probe intensity and lifetime in the SWIR window promises to enhance current *in vivo* optical molecular imaging applications at the mesoscopic and macroscopic scales by combining gain in imaging resolution to better resolve the biodistribution of probes with monitoring multiple processes or additional molecular information via lifetime sensing. However, limitations in detection hardware and lack of suitable SWIR probes remain a challenge in the translation from NIR to SWIR imaging. Herein, we report a quantitative comparison between brightness and lifetime measurements of two conventional NIR probes and two commercially available SWIR probes in the SWIR imaging window. The fluorescent signal for all probes was detectable at clinically relevant concentrations, where the NIR probes yielded a higher intensity compared to the SWIR probes. Although a direct comparison between the brightness of IRDye800CW and IR-E1050 has been previously reported showing IRDye800CW being brighter in the SWIR window,[2] we show that NIR probe AF750 outperforms the SWIR fluorophores in brightness, noting that its peak emission is blue-shifted compared to that of IRDye800CW.

It is noteworthy that fluorescent temporal decays were readily acquired beyond 1000 nm with good SNR given the still relatively low quantum efficiency of our SPAD array in the SWIR window (QE $\sim$ 5% at 1000 μm, spectral response reported in Ref. 16). The decent photon counts acquired on relatively low concentration samples related to the short IRF associated with the SPAD array ($\sim$120 ps) enabled to quantify lifetimes with good accuracy. Still, this study should benefit from the implementation of detectors with higher QE in the SWIR, such as the germanium-based SPAD detectors. To our knowledge, this is the first report on the lifetimes of these two SWIR fluorophores. Characterizing the fluorescent lifetime of the SWIR probes further shows the current superiority in the applicability of the NIR probes. Shorter fluorescence lifetime requires detectors with higher temporal resolution for effective detection as well as increased experimental control to ensure temporal stability (reduce drift and jitter). Moreover, for *in vivo* applications, shorter lifetimes estimation can be affected by the topography of the boundary condition as well as the depth of the fluorescence inclusion. Hence, quantifying short lifetime robustly is more difficult at large and requires increased expertise.

Overall, these results complement the previous characterization of conventional NIR fluorophores. It has been previously demonstrated that these fluorophores emit fluorescent signal well into the SWIR window similarly to the ones presented herein, where the signal is detected even when excited at a non-optimal wavelength.[5] We further extended this work by demonstrating the effective detection of fluorescent lifetime with a SPAD array optimized for measurements in the VIS-NIR window. In turn, this lifetime information was used for quantifying the fluorophore fraction of well-controlled mixtures. These results pave the way for lifetime multiplexing in the SWIR window using the vast library of conventional NIR fluorophores and single excitation wavelength, which should provide invaluable information in preclinical studies until suitable SWIR fluorophores become available.

In summary, the experimental results show that the conventional NIR-excited fluorophores outperformed the commercially available SWIR probes in both brightness and lifetime in the SWIR window. Furthermore, effective detection of both lifetime and intensity of tail emission in the SWIR window shows promise for the translation of multimodal fluorescence imaging into the SWIR region with the current library of NIR fluorophores. Hence, this study demonstrates the feasibility of lifetime multiplexing in the SWIR range using the tail emission of conventional fluorophores over current commercially available organic SWIR-specific probes.

Disclosures

The authors declare that there are no conflicts of interest.

Acknowledgments

This work was supported by the following grants from the National Institutes of Health (Grant Nos. R01CA207725, R01CA237267, and R01CA250636).

Code, Data, and Materials Availability

All analyses are performed using freely available software.[20] Data underlying the results presented in this paper are not publicly available at this time but may be obtained from the authors upon reasonable request.

References

1. D. Faulkner et al., *Diffuse Fluorescence Tomography*, ch. 11, pp. 11–1–11–28, AIP Publishing LLC, Melville, New York (2021).
2. J. A. Carr et al., "Shortwave infrared fluorescence imaging with the clinically approved near-infrared dye indocyanine green," *Proc. Natl. Acad. Sci. U. S. A.* **115**(17), 4465–4470 (2018).
3. O. T. Bruns et al., "Next-generation in vivo optical imaging with short-wave infrared quantum dots," *Nat. Biomed. Eng.* **1**, 0056 (2017).
4. B. Li et al., "Organic NIR-II molecule with long blood half-life for in vivo dynamic vascular imaging," *Nat. Commun.* **11**(1), 1–11 (2020).
5. B. K. Byrd et al., "Characterizing short-wave infrared fluorescence of conventional near-infrared fluorophores," *J. Biomed. Opt.* **24**(3), 035004 (2019).
6. R. I. Dmitriev, X. Intes, and M. M. Barroso, "Luminescence lifetime imaging of three-dimensional biological objects," *J. Cell Sci.* **134**(9), 1–17 (2021).
7. M. Wang et al., "Rapid diagnosis and intraoperative margin assessment of human lung cancer with fluorescence lifetime imaging microscopy," *BBA Clin.* **8**, 7–13 (2017).
8. H.-J. Lin, P. Herman, and J. R. Lakowicz, "Fluorescence lifetime-resolved pH imaging of living cells," *Cytometry Part A* **52A**(2), 77–89 (2003).
9. A. Rudkouskaya et al., "Quantification of trastuzumab–HER2 engagement in vitro and in vivo," *Molecules* **25**(24), 5976 (2020).
10. M. Ochoa et al., *Macroscopic Fluorescence Lifetime Imaging for Monitoring of Drug–Target Engagement*, pp. 837–856, Springer US, New York (2022).
11. S. Gao et al., "Design and characterization of a time-domain optical tomography platform for mesoscopic lifetime imaging," *Biomed. Opt. Express* **13**(9), 4637–4651 (2022).
12. Y. Fan et al., "Lifetime-engineered nir-ii nanoparticles unlock multiplexed in vivo imaging," *Nat. Nanotechnol.* **13**(10), 941–946 (2018).
13. M. Y. Berezin and S. Achilefu, "Fluorescence lifetime measurements and biological imaging," *Chem. Rev.* **110**(5), 2641–2684 (2010).
14. Y. Mu, V. Pera, and M. Niedre, "Multiplexed fluorescence mediated tomography with temporal and spectral data," *J. Biomed. Opt.* **21**(10), 105001 (2016).
15. F. Thorburn et al., "Ge-on-si single-photon avalanche diode detectors for short-wave infrared wavelengths," *J. Phys.: Photonics* **4**(1), 012001 (2021).
16. F. Ceccarelli et al., "Red-enhanced photon detection module featuring a 32 × 1 single-photon avalanche diode array," *IEEE Photonics Technol. Lett.* **30**(6), 557–560 (2018).
17. P. Vines et al., "High performance planar germanium-on-silicon single-photon avalanche diode detectors," *Nat. Commun.* **10**(1), 1086 (2019).
18. C. M. Natarajan, M. G. Tanner, and R. H. Hadfield, "Superconducting nanowire single-photon detectors: physics and applications," *Supercond. Sci. Technol.* **25**(6), 063001 (2012).
19. J. Yu et al., "Intravital confocal fluorescence lifetime imaging microscopy in the second near-infrared window," *Opt. Lett.* **45**(12), 3305–3308 (2020).

20. S.-J. Chen et al., "In vitro and in vivo phasor analysis of stoichiometry and pharmacokinetics using short-lifetime near-infrared dyes and time-gated imaging," *J. Biophotonics* **12**(3), e201800185 (2019).
21. J. T. Smith et al., "In vitro and in vivo nir fluorescence lifetime imaging with a time-gated spad camera," *Optica* **9**, 532–544 (2022).

Xavier Intes received his PhD from the Université de Bretagne Occidentale and postdoctoral training at the University of Pennsylvania. Currently, he is working as a professor in the Department of Biomedical Engineering, Rensselaer Polytechnic Institute. He is also an AIMBE/SPIE/Optica fellow. He acted as the chief scientist of Advanced Research Technologies Inc. His research interests include the application of diffuse functional and molecular optical techniques for biomedical imaging in preclinical and clinical settings.

Biographies of the other authors are not available.